A Letters Journal Exploring the Frontiers of Physics

September 2007

EPL, **79** (2007) 64003
doi: 10.1209/0295-5075/79/64003

www.epljournal.org

Synchronization via clustering in a small delay-coupled laser network

C. M. González, C. Masoller, M. C. Torrent and J. García-Ojalvo

Departament de Física i Enginyeria Nuclear, Universitat Politècnica de Catalunya - Colom 11, E-08222 Terrassa, Barcelona, Spain

received 12 May 2007; accepted in final form 3 August 2007
published online 3 September 2007

PACS 42.65.Sf – Dynamics of nonlinear optical systems; optical instabilities, optical chaos and complexity, and optical spatio-temporal dynamics
PACS 05.45.Xt – Synchronization; coupled oscillators
PACS 42.55.Px – Semiconductor lasers; laser diodes

Abstract – We study experimentally how synchronization emerges in a small network of delay-coupled lasers, as the coupling strength increases. Specifically, we optically couple three semiconductor lasers to each other via an external mirror. The system exhibits natural mismatches between its three elements, and is designed so that the coupling delays and strengths are non-uniform throughout the network. For weak coupling a cluster arises where two lasers synchronize their low-frequency dynamics; for stronger coupling all three lasers synchronize. A simple model gives good agreement with the experimental observations.

Introduction. – Synchronization is a fascinating example of emerging dynamics in coupled oscillators, and plays an important functional role in the collective dynamical behavior of complex systems [1–3]. The effect of time-delayed interactions, which arise from a realistic consideration of finite communication times, is a key issue that has received considerable attention. Some delay-induced phenomena such as multi-stability [4,5], oscillation death [6,7], and discretization of frequencies [8,9] are now well known. However, the mechanisms by which two or more distant oscillators synchronize in the presence of non-negligible delays in their interactions remain poorly understood.

Coupled semiconductor lasers are excellent devices for studying the mechanisms of emergence of synchrony because they are inexpensive, reliable, and their intrinsic behavior is well understood [10,11]. Recently, zero-lag isochronous synchronization was reported, experimentally and theoretically, in linear arrays of three coupled lasers [12–14]. In these studies the delay times between the lasers were adjusted to be equal; however, it is also important to understand how a system of coupled oscillators synchronizes when the delays in the interactions are different for the different oscillators. Non-uniform, distributed time delays arise naturally in coupled systems, and several authors have reported that they can have a stabilizing effect [15–18].

Here we study the influence of non-uniform coupling strengths and non-uniform delay times on the onset of synchronization in an experimental system consisting of three semiconductor lasers mutually coupled through an external mirror. Our results show that synchronization arises via the formation of two-laser clusters. This observation is in good agreement with a simple theoretical model. Clustering has been studied theoretically [19–21] and experimentally [22–24] in large ensembles of coupled oscillators. Recently, Rogister and Roy [25] studied a square array of lasers (50×50) with homogeneous local coupling without delay, finding that the synchronization of the lasers of the array resulted in localized excitations, wandering along well-defined trajectories. The experimental system presented here could allow for a systematic analysis of the emergence of those behaviors in a simpler small array. Our results can also have broad applications to other systems, such as small networks of coupled neurons.

Experimental setup. – A schematic diagram of the experimental setup is displayed in fig. 1. Three semiconductor lasers (LD1, LD2, and LD3, AlGaInP index-guided and multi-quantum well devices, Sharp GHO65010B2A) are mutually coupled through their lasing fields via an external mirror (M), which also supplies optical feedback to each laser. The lasers operate in a single longitudinal mode with a nominal wavelength of 654 nm

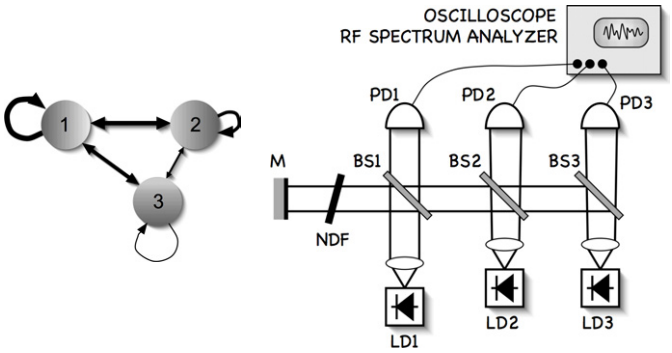

Fig. 1: Left, scheme of the network studied. Note the different width of the lines, indicating different strength of the optical coupling. Right, experimental setup: LD, laser diodes; BS, beamsplitters; M, mirror; NDF, neutral density filter; PD, photodetectors.

when operating in isolation. The temperature and pump current of the lasers are controlled with an accuracy of $\pm 0.01\,^{\circ}\mathrm{C}$ and $\pm 0.1\,\mathrm{mA}$, respectively. At temperatures $T_{\mathrm{LD1}} = 19.76\,^{\circ}\mathrm{C}$, $T_{\mathrm{LD2}} = 18.53\,^{\circ}\mathrm{C}$, and $T_{\mathrm{LD3}} = 18.32\,^{\circ}\mathrm{C}$, the threshold currents of the lasers (when isolated) are $I^{\mathrm{th}}_{\mathrm{LD1}} = 31.61\,\mathrm{mA}$, $I^{\mathrm{th}}_{\mathrm{LD2}} = 28.87\,\mathrm{mA}$, and $I^{\mathrm{th}}_{\mathrm{LD3}} = 31.15\,\mathrm{mA}$. The operating currents are set to $I_{\mathrm{LD1}} = 32.77\,\mathrm{mA}$, $I_{\mathrm{LD2}} = 30.00\,\mathrm{mA}$, and $I_{\mathrm{LD3}} = 32.10\,\mathrm{mA}$.

Three beam splitters with 50% transmittance (BS1, BS2 and BS3) couple the lasers with each other through the common reflected light of the external mirror. In this geometrical arrangement the feedback delay times are $\tau_{11} = 5.43\,\mathrm{ns}$, $\tau_{22} = 4.8\,\mathrm{ns}$, and $\tau_{33} = 7.3\,\mathrm{ns}$; and the flight times between the lasers (coupling times) are: $\tau_{12} = 5.06\,\mathrm{ns}$, $\tau_{13} = 6.4\,\mathrm{ns}$, and $\tau_{23} = 6.03\,\mathrm{ns}$. The amount of light injected into the lasers is controlled by a neutral density filter (NDF) located in front of the mirror. We note that the coupling strengths between the lasers and the optical feedback strengths are not controlled separately, but are all related and controlled with the filter.

The detection of the laser outputs is achieved by fast photodetectors of 1 GHz bandwidth (Thorlabs DET210)[1]. The received signal is sent simultaneously to a 1 GHz oscilloscope (DS06104A Agilent), and to a spectrum analyzer (Anritsu MS2651B) via two amplifiers (2 GHz, Femto high-speed amplifier). We note that the two input channels of the oscilloscope allow the detection of only two laser outputs simultaneously.

Each laser operates, in the absence of coupling with the other two, in the low-frequency fluctuation (LFF) regime, induced by its own optical feedback from the external mirror. The laser intensities and the RF spectra are displayed in fig. 2. The LFF regime consists of sudden power dropouts followed by gradual, stepwise recoveries. These dropouts are the envelope of a much faster pulsing dynamics that cannot be observed with 1 GHz bandwidth detectors [26]. The mean time interval between dropouts is approximately 200 ns, 100 ns and 150 ns for LD1, LD2 and LD3, respectively. The frequency of the dropouts is different for each laser, because their operating and feedback conditions vary among the three lasers. The operating conditions are slightly different because the temperature and the injection currents of the lasers are adjusted to match their optical frequencies as closely as possible, in order to have the strongest mutual optical coupling. The feedback conditions are also different, due to the heterogeneous geometry of the setup: it can been noticed that the light fed back into laser LD1 passes only one beam-splitter (BS1), while the light fed back into laser LD2 (LD3) passes two (three) beam splitters. The feedback delay times are different for each laser as well, and we note that the laser with the strongest feedback is LD1 while the laser with larger feedback time is LD3.

Route to synchronization. – We now examine how synchronization arises in this system as the optical coupling between the lasers strengthens. Synchronous behavior will be defined in terms of the mutual occurrence of power dropouts, which act as low-frequency markers of the lasers' dynamics. The coupling strength is controlled by the NDF filter located in front of the mirror. When the filter absorbs 40% of the incident light, coupling is weak and a clustering state arises in which only two lasers, LD1 and LD3, synchronize their dropouts (fig. 3, left), while laser LD2 drops independently of the other two. Without the NDF filter, the mutual coupling is stronger and all three lasers adjust their dynamics to drop out together (fig. 4, left).

Even if the dropouts are synchronized, they are not necessarily simultaneous: there are delay times associated with both the couplings and feedbacks, as mentioned above. In order to determine the lag times between the synchronized lasers, we compared the times when dropouts occur in the intensities of laser pairs. In the cluster regime, LD1 and LD3 drop almost simultaneously (fig. 3(d)). Thus, the lasers that form the cluster synchronize in this case with almost zero lag. In the synchronized regime arising at larger coupling, LD1 and LD3 dropouts occur also with almost zero lag time (fig. 4(b)), while LD2 dropouts occur about 10 ns earlier (fig. 4(d)).

Figure 5 provides insight into how synchronization develops in the frequency domain, by depicting the RF-spectra of the clustered and synchronization states. Clearly, the clustered lasers lock almost all frequency peaks in their spectra, specially the lowest frequency peak corresponding to the low-frequency fluctuations (figure inset). This contrasts with what happens with LD2, where the overlapping is very poor, particularly at the LFF peak (inset). In the synchronized state, on the other hand, all lasers show a substantial overlap in the whole RF-frequency spectrum.

Experimentally we observe that the choice of lasers integrating the cluster depends on the coupling strengths

[1]Photodetectors PD1 and PD2 receive light from more than one laser, but the signals from the lasers facing them (LD1 and LD2, respectively) dominate.

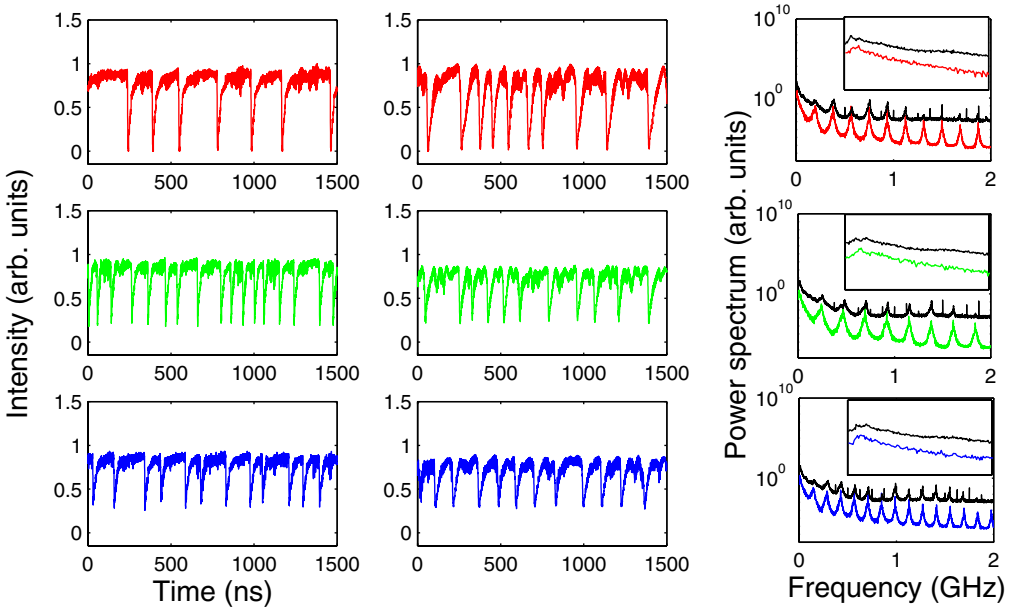

Fig. 2: LFF dynamics in the absence of coupling: LD1 (top row), LD2 (middle row) and LD3 (bottom row). Left column: experimentally observed intensities; center column: numerically calculated intensities; right column: experimental (top traces) and numerical (bottom traces) RF-spectra. The insets display the low-frequency peak (the horizontal axis span 0.1 GHz). The scale of the vertical axis is such that the size of the dropouts of laser LD1 is 1. The numerically calculated spectra are shifted vertically for clarity. The coupling parameters used in the simulations are $\eta_{11} = 31.6\,\mathrm{ns}^{-1}$, $\eta_{22} = 22.3\,\mathrm{ns}^{-1}$, and $\eta_{33} = 20\,\mathrm{ns}^{-1}$. Other parameters are indicated in the text.

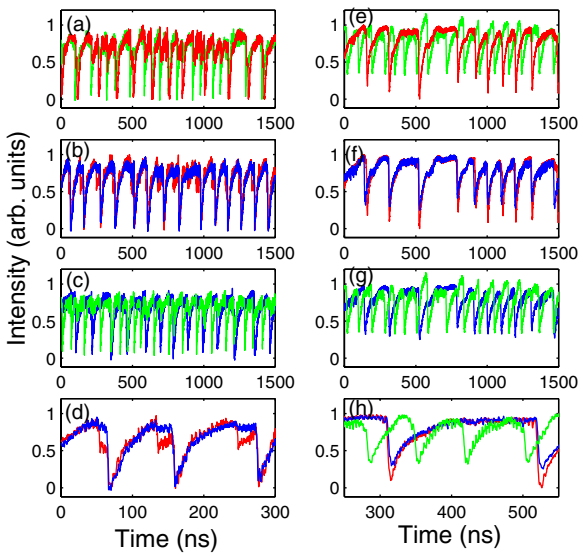

Fig. 3: Dynamics in the clustering state: LD1 and LD2 (a,e), LD1 and LD3 (b,f) and LD2 and LD3 (c,g). The laser pairs are not monitored simultaneously. Panels (d,h) are zoomed-in versions of (b,f). Left column: experimentally observed intensities; right column: numerically calculated intensities. The feedback and coupling parameters are $\eta_{11} = 26.4\,\mathrm{ns}^{-1}$, $\eta_{22} = 18.7\,\mathrm{ns}^{-1}$, $\eta_{33} = 16.7\,\mathrm{ns}^{-1}$, $\eta_{12} = 7.2\,\mathrm{ns}^{-1}$, $\eta_{13} = 5.9\,\mathrm{ns}^{-1}$, and $\eta_{23} = 5.6\,\mathrm{ns}^{-1}$. The frequency shifts are $\omega_1 = 0$, $\omega_2 = 5$, and $\omega_3 = -5\,\mathrm{rad/ns}^{-1}$. Other parameters are indicated in the text.

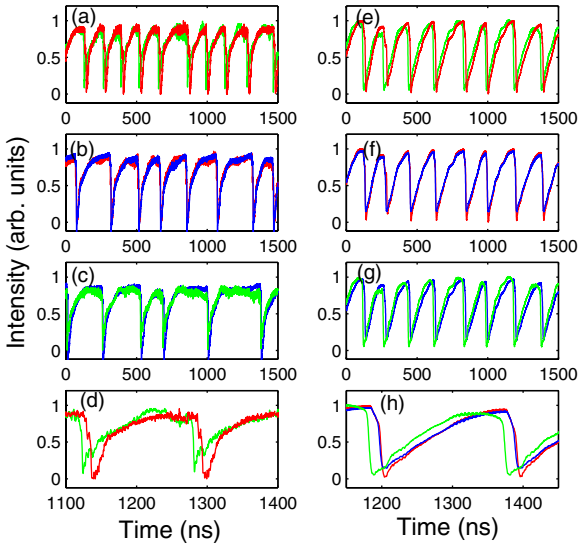

Fig. 4: Dynamics in the synchronization state: LD1 and LD2 (a,e), LD1 and LD3 (b,f) and LD2 and LD3 (c,g). The laser pairs are not monitored simultaneously. Panels (d,h) are zoomed-in versions of (b,f). Left column: experimentally observed intensities; right column: numerically calculated intensities. The feedback parameters are as in fig. 2 and the coupling parameters are $\eta_{12} = 22.9\,\mathrm{ns}^{-1}$, $\eta_{13} = 18.7\,\mathrm{ns}^{-1}$, and $\eta_{23} = 17.7\,\mathrm{ns}^{-1}$. The detunings are as in fig. 3. Other parameters are indicated in the text.

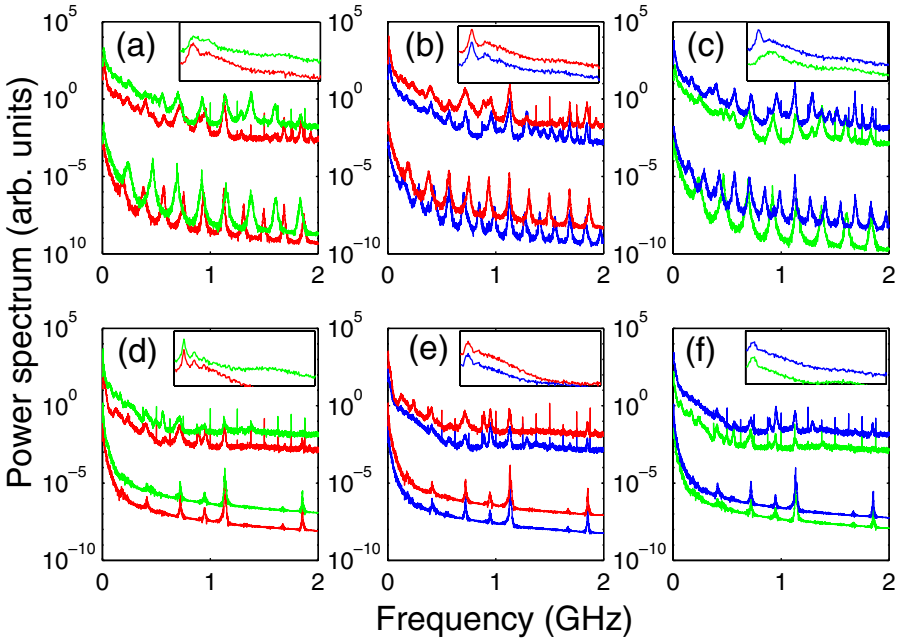

Fig. 5: Experimental (top lines) and numerical (bottom lines) RF-spectra in the clustering state (top row) and in the synchronized state (bottom row). (a,d) LD1 and LD2; (b,e) LD1 and LD3; (c,f) LD2 and LD3. The insets display the low-frequency peak (the horizontal scale is 0.1 GHz).

in the network. When an additional NDF filter is located between LD1 and BS1, diminishing the injection and feedback strengths of LD1, a cluster is formed by LD1 and LD2 (results not shown), with a lag time of around 5 ns, which is again maintained in the fully synchronized regime.

Numerical simulations. – We have performed simulations based on a model that takes into account the effects of optical feedback and mutual optical injection [27,28]. Extensive simulations unveil a rich variety of dynamical regimes and demonstrate that the clustered and the synchronized behaviors also occur when there are parameter mismatches between the lasers. For the sake of simplicity, in this letter we describe the dynamics of the array assuming that the laser parameters are identical. The equations for the slowly-varying complex amplitude, $\mathcal{E}_i$, and the carrier density, $\mathcal{N}_i$, in the i-th laser read

$$\dot{\mathcal{E}}_i = i\omega_i\mathcal{E}_i + k(1+i\alpha)(\mathcal{N}_i-1)\mathcal{E}_i + \sqrt{D}\xi_i(t) + \sum_{j=1}^{3}\eta_{ij}\mathcal{E}_j(t-\tau_{ij})\exp(-i\omega_0\tau_{ij}), \quad (1)$$

$$\dot{\mathcal{N}}_i = \gamma_n(\mathcal{I}-\mathcal{N}_i-\mathcal{N}_i|\mathcal{E}_i|^2), \quad (2)$$

where ω_i is the solitary frequency of laser i-th (that is, in the absence of feedback or coupling), relative to a common reference frequency, ω_0. α is the linewidth enhancement factor, k is the cavity loss coefficient, γ_n is the carrier decay rate, η_{ij} is the coupling coefficient between lasers LDi and LDj (η_{ii} being the self-feedback coefficient), $\mathcal{I}$ is the pump parameter (the threshold being $\mathcal{I}_{\rm th}=1$ in the absence of feedback and coupling), D is the spontaneous emission strength and ξ_i are uncorrelated Gaussian white noises with zero mean. The pump parameter and the delay times are comparable to those used in the experiments: $\mathcal{I}=1.037$, $\tau_{11}=5.3$ ns, $\tau_{22}=4.3$ ns, and $\tau_{33}=7.1$ ns, $\tau_{12}=4.8$ ns, $\tau_{13}=6.2$ ns, and $\tau_{23}=5.7$ ns. The internal laser parameters are $k=250\,\mathrm{ns}^{-1}$, $\alpha=4$, $\gamma_n=0.6\,\mathrm{ns}^{-1}$, $D=10^{-5}\,\mathrm{ns}^{-1}$, and $\omega_0=2\pi c/\lambda_0$, where c is the speed of light in vacuum and $\lambda_0=654$ nm.

In the simulations we observe that a cluster usually develops before the three lasers synchronize, with the feedback strengths, the coupling strengths, and the relative detunings among the lasers determining which lasers integrate the cluster. Figures 2, 3 and 4 compare the experimental data discussed above with results from numerical simulations, in which the intensities were filtered to simulate the bandwidth of the detectors, and normalized such that the amplitude of the dropouts of laser LD1 is 1. The feedback coefficients η_{ii} used in the simulations take into account the fact that the laser LD1 (LD3) has the strongest (weakest) feedback. The coupling parameters (which are considered symmetric, $\eta_{ij}=\eta_{ji}$) take into account that lasers LD1-LD2 (LD2-LD3) have the strongest (weakest) coupling. It is worth noticing that in the experiment, different alignment quality can make the coupling strengths not only quite arbitrary but also asymmetric.

For the choice of lasers integrating the cluster, two mechanisms seem to be relevant and compete. On the one hand, the lasers that have more similar optical injection (feedback and coupling) tend to cluster. In the absence of detunings, it is observed that as the coupling increases, LD2 and LD3, or LD1 and LD2, cluster before all three lasers synchronize (results not shown). On the other hand, if one of the lasers is weakly coupled to the other two, or if two lasers are more strongly coupled, often the strongly coupled lasers are the ones forming the cluster.

In the simulations, coupling among the lasers was adjusted by variations of the frequency detunings and the coupling coefficients, the latter depending on the optical alignment. As an example, fig. 3 displays a cluster formed by LD1 and LD3, that is observed when LD3 has negative detuning with respect to LD1. A simple interpretation of the observed cluster is the following: the external optical injection (feedback + coupling) modifies the lasers optical frequencies, and roughly speaking, the frequencies shift towards negative values, with the shifts being proportional to the total injection strengths. Since LD3 is the laser that has *less* injection, its frequency shift is less than that of LD1 (which has the strongest injection), and an extra negative detuning is needed to move the LD2 frequency closer to that of LD1.

In the intensity power spectra we can observe the synchronization mechanism in the frequency domain. Without mutual coupling (fig. 2, right column), the spectrum of each laser consists of a dominant peak at a low frequency (the inverse of this frequency is the average dropout period), and harmonics separated by the external cavity frequency, $1/\tau_{ii}$. Since the average dropout period is different for the different lasers, the main peaks are at different frequencies. Moreover, since the delay times τ_{ii} are also different, the harmonic peaks are located at different frequencies. When the lasers are coupled but the coupling is weak (fig. 5, top row), the numerical spectra show that the frequencies begin to adjust both in the low and high frequency ranges: some harmonics begin to disappear, while others "move" such that they overlap. For larger feedback and coupling (fig. 5, bottom row), the spectra of the lasers synchronize at both low and high frequencies. The same process of frequency selection, where some peaks vanish and others "move" (in a sort of frequency pulling phenomenon occurring in the RF spectrum), is observed experimentally.

Discussion. – We have experimentally studied the emergence of synchronization in a small network of three semiconductor lasers coupled with distributed delay times. Our results show that clusters emerge generically as the system tends towards complete synchronization for increasing coupling strength. The clustering is associated with an overlap of some of the peaks in the RF spectrum.

The experimental observations are satisfactorily reproduced by a rate equation model of the Lang-Kobayashi type. The model, presented in eqs. (1), (2), is valid for a laser emitting in a single longitudinal mode. The lasers in the experiments emit multiple longitudinal modes, and yet the agreement between the experiment and the model predictions is surprisingly good. This can be explained as due to the out-of-phase dynamics of the longitudinal modes. Because of the competition for the common carrier reservoir, the longitudinal modes oscillate in antiphase, such that the total output (that is, the sum of the modal intensities) is similar to that of a single-mode laser.

* * *

We thank J. M. Buldú by suggestions regarding the design of the experimental setup. This research was supported by the Ministerio de Educacion y Ciencia (Spain) under projects FIS2005-07931-C03-03 and FIS2006-11452, by the Generalitat de Catalunya, and by the GABA project (European Commission, FP6-NEST contract 043309).

REFERENCES

[1] Boccaletti S., Kurths J., Osipov G., Valladares D. L. and Zhou C. S., *Phys. Rep.*, **1** (2002) 366.
[2] Pikovsky A., Rosenblum M. and Kurths J., *Synchronization: A Universal Concept in Nonlinear Sciences* (Cambridge University Press, Cambridge, England) 2003.
[3] Manrubia S., Mikhailov A. S. and Zanette D. H., *Emergence of Dynamical Order* (World Scientific, Singapore) 2004.
[4] Schuster H. G. and Wagner P., *Prog. Theor. Phys.*, **81** (1989) 939.
[5] Yeung M. K. S. and Strogatz S. H., *Phys. Rev. Lett.*, **28** (1999) 648.
[6] Reddy D. V. R., Sen A. and Johnston G. L., *Phys. Rev. Lett.*, **80** (1998) 5109.
[7] Herrero R., Figueras M., Rius J., Pi F. and Orriols G., *Phys. Rev. Lett.*, **84** (2000) 5312.
[8] Yanchuk S., *Phys. Rev. E*, **72** (2005) 036205.
[9] Wunsche H.-J., Bauer S., Kreissl J., Ushakov O., Korneyev N., Henneberger F., Wille E., Erzgraber H., Peil M., Elsaber W. and Fischer I., *Phys. Rev. Lett.*, **94** (2005) 163901.
[10] Kim M. Y., Roy R., Aron J. L., Carr T. W. and Schwartz I. B., *Phys. Rev. Lett.*, **94** (2005) 088101.
[11] Buldu J. M., Heil T., Fischer I., Torrent M. C. and García-Ojalvo J., *Phys. Rev. Lett.*, **96** (2006) 024102.
[12] Sivaprakasam S., Paul J., Spencer P. S., Rees P. and Shore K. A., *Opt. Lett.*, **28** (2003) 1397.
[13] Fischer I., Vicente R., Buldu J. M., Peil M., Mirasso C. R., Torrent M. C. and García-Ojalvo J., *Phys. Rev. Lett.*, **97** (2006) 123902.
[14] Lee M. W., Paul J., Masoller C. and Shore K. A., *J. Opt. Soc. Am. B*, **23** (2006) 846.
[15] Atay F. M., *Phys. Rev. Lett.*, **91** (2003) 094101.
[16] Huber D. and Tsimring L. S., *Phys. Rev. E*, **71** (2005) 036150.
[17] Eurich C. W., Thiel A. and Fahse L., *Phys. Rev. Lett.*, **94** (2005) 158104.

[18] Masoller C. and Marti A. C., *Phys. Rev. Lett.*, **94** (2005) 134102.
[19] Nakamura Y., Tominaga F. and Munakata T., *Phys. Rev. E*, **49** (1994) 4849.
[20] Manrubia S. C. and Mikhailov A. S., *Phys. Rev. E*, **60** (1999) 1579.
[21] Park S. H., Kim S., Pyo H. B. and Lee S., *Phys. Rev. E*, **60** (1999) 4962.
[22] Wang W., Kiss I. Z. and Hudson J. L., *Chaos*, **10** (2000) 248.
[23] Otsuka K., Ohtomo T., Maniwa T., Kawasaki H. and Ko J. Y., *Chaos*, **13** (2003) 1014.
[24] Tanguy Y., Houlihan J., Huyet G., Viktorov E. A. and Mandel P., *Phys. Rev. Lett.*, **96** (2006) 053902.
[25] Rogister F. and Roy R., *Phys. Rev. Lett.*, **98** (2007) 104101.
[26] Fischer I., van Tartwijk G. H. M., Levine A. M., Elsässer W., Göbel E. and Lentra D., *Phys. Rev. Lett.*, **76** (1996) 220.
[27] García-Ojalvo J., Casademont J., Mirasso C. R., Torrent M. C. and Sancho J. M., *Int. J. Bifurcat. Chaos*, **9** (1999) 2225.
[28] Kozyreff G., Vladimirov A. G. and Mandel P., *Phys. Rev. Lett.*, **85** (2000) 3809.